ICES Journal of Marine Science, 55: 905–917. 1998
Article No. jm980353

A split-beam echo counting model: development of statistical procedures

T. J. Mulligan and D. G. Chen

Mulligan, T. J., and Chen, D. G. 1998. A split-beam echo counting model: development of statistical procedures. – ICES Journal of Marine Science, 55: 905–917.

Mulligan and Kieser (1996) (ICES Journal of Marine Science, 53: 403–406) proposed a split-beam echo counting model that addressed the problem of non-uniform detection probability combined with non-uniform fish density over the beam cross-section. To apply the model to real data, statistical procedures to estimate three-dimensional density functions, to estimate kernel density smoothing parameters from the data, and to estimate a data-based smoothing parameter for kernel regression have been developed. In addition, a method to select echoes from individual fish that have been accurately tracked by the automatic tracking algorithm is described. The performance of the model was tested using data from a simulation program and from an experiment that compared acoustic estimates with visual counts of migrating salmon.

Key words: echo density, fish density, fish flux, fish migration speed, fish detection probability, kernel density estimation, kernel regression estimation, smoothing parameter selection.

Received 2 June 1997; accepted 18 January 1998.

T. J. Mulligan, and D. G. Chen: Government of Canada Department of Fisheries and Oceans, Pacific Biological Station, Nanaimo, B.C. V9R 5K6, Canada. Correspondence to T. J. Mulligan: tel: +1 250 7567039; fax: +1 250 7567053; e-mail: mulligant@dfo-mpo.gc.ca

Introduction

A split-beam acoustic system is being used on the Fraser River in British Columbia, Canada to estimate the number of salmon that migrate upstream past the acoustic monitoring site. The system is configured to look sideways from the bank towards the middle of the river. Upstream migrating adult salmon prefer to swim close to the bottom, where the current is lower. This results in a variable fish density over the acoustic beam cross-section. An empirical, stochastic echo counting model was developed by Mulligan and Kieser (1996) to examine this issue. The model exploits the unique ability of a split-beam system to measure the three-dimensional location of targets and to track the trajectories of individual fish. It addresses the problem of non-uniform detection probability combined with non-uniform fish density over the beam cross-section. The model estimates the number of migrating salmon by combining information from the observed echo distribution of both tracked and untracked fish, the trajectories of tracked fish, and the measured fish detection probability. In this paper we discuss the development and implementation of the mathematical and statistical procedures for this model.

Non-parametric estimation methods were used in the model as this allowed greater flexibility in describing data from a wide variety of distributions. Kernel density estimation was used to describe the functional dependence of echo density on location and kernel regression was used to describe the fish detection probability. Published references for these statistical procedures were inadequate to meet the needs of the model. Therefore, we have extended one-dimensional kernel density estimation techniques to three dimensions and have derived independent smoothing parameter selection for this case. We describe how these smoothing parameters can be estimated from the data for both kernel density estimation and kernel regression.

The model performance was tested using both simulated and real data. Performance testing helped in the selection and development of reliable statistical procedures and gave a measure of the bias and variance of the model estimates. The simulated data follow the model equations and satisfy the model's assumptions. The real data come from an experiment conducted at a

1054–3139/98/050905+13 $30.00/0

site on the Thompson River near Spences Bridge, British Columbia. This experiment compared acoustic estimates with a simultaneous visual count of the number of migrating fish (Enzenhofer *et al.*, 1998). Reliable estimates from the Spences Bridge data required the development of a method to remove echoes from sources other than migrating fish and a method to select only well-tracked individual fish echoes from the set of all tracked fish echoes.

Split-beam echo counting model

When salmon swim through the acoustic beam, there are three possibilities for generating echoes: (1) the fish may pass through the beam and no echo is detected; (2) the fish may be detected by generating one or more echoes, but not be tracked by the target tracking algorithm; and (3) the fish may generate several echoes and be tracked. (Our fish tracking software is typically configured to require a minimum of four echoes from each tracked target.) Thus, there are echoes from both tracked and untracked fish recorded by the acoustic system. There are also fish that pass through the beam and are not detected. The echo counting model described below is designed to account for these three possibilities.

We will use the same coordinate systems as Mulligan and Kieser (1996) – see the Appendix for details. The Cartesian coordinates used in the equations below can be briefly described as follows: The z-axis is located along the acoustic beam axis with the origin at the front face of the transducer. The x-axis represents the upstream/downstream direction with positive x-values in the downstream direction. The y-axis represents the river surface/bottom direction with positive y values in the surface direction. The model defines a "fish flux" as the product of fish density times migration speed. The estimate of the number of fish migrating through the acoustic beam is obtained from the integration of this flux over the vertical longitudinal cross-section of the beam and over the elapsed time. This is based on the assumption that the fish density function, detection probability function, and echo density function are approximately time-independent for the duration of the data collection. A detailed derivation of the model and a description of the data required for its implementation is given in Mulligan and Kieser (1996). A brief summary is given below.

The process begins by relating the fish density to the observed echoes. The observed cumulative echo density is given by:

$$e(x,y,z) = \rho(x,y,z)p(x,y,z)I \tag{1}$$

where $e(x,y,z)$ is the cumulative echo density in units of echoes $\times$ m^{-3}, $\rho(x,y,z)$ is the fish density in units of fish $\times$ m^{-3}, $p(x,y,z)$ is the echo detection probability in units of echoes $\times$ fish^{-1} $\times$ ping^{-1}, and I is the number of acoustic transmission in units of pings.

Equation (1) describes a stochastic process where the terms $e(x,y,z)$, $\rho(x,y,z)$, and $p(x,y,z)$ are random variables with $\rho(x,y,z)$ and $p(x,y,z)$, assumed to be independent. Therefore the expectation for $e(x,y,z)$ is:

$$E[e(x,y,z)] = E[\rho(x,y,z)] \times E[p(x,y,z)] \times I,$$

which leads to:

$$E[\rho(x,y,z)] = \frac{E[e(x,y,z)]}{I \times E[p(x,y,z)]}. \tag{2}$$

Equation (2) can then be expressed in terms of estimated functions based on the data as:

$$\hat{\rho}(x,y,z) = \frac{\hat{e}(x,y,z)}{I \times \hat{p}(x,y,z)}, \tag{3}$$

where $\hat{e}(x,y,z)$ is estimated from all fish echoes and $\hat{p}(x,y,z)$ is estimated from a separate set of measurements using a single fish suspended from a target frame (see the section describing the estimation of the detection probability function).

Next, the fish migration speed, $S(x,y,z)$, and the fraction of fish migrating upstream, $f_u(x,y,z)$, are estimated using the subset of the original observations that come from tracked fish. The speed is combined with the estimated density and fraction of upstream migrants to obtain an estimate of the fish flux, α, given by:

$$\hat{\alpha}(y,z) = \hat{\rho}(0,y,z) \times \hat{S}(0,y,z) \times \hat{f}_u(0,y,z), \tag{4}$$

where α is estimated over the (y,z) plane at $x = 0$. Finally, the number of fish migrating past the site, N, is estimated by:

$$\hat{N} = (T_2 - T_1) \times \int\int \hat{\alpha}(y,z)dydz, \tag{5}$$

where T_1 and T_2 are the start and end times, respectively, for the data collection.

Simulation program

To test the performance of the model, a simulation computer program was written that obeyed Equation (1), while allowing stochastic variation in several of the variables. Simulated fish pass through the beam one at a time. Each fish has a random starting location, direction of movement, and migration speed (Fig. 1). The simulated data are not meant to mimic the true fish migration with respect to their time dependence; however, they do mimic the spatial dependence. We use the simulated data

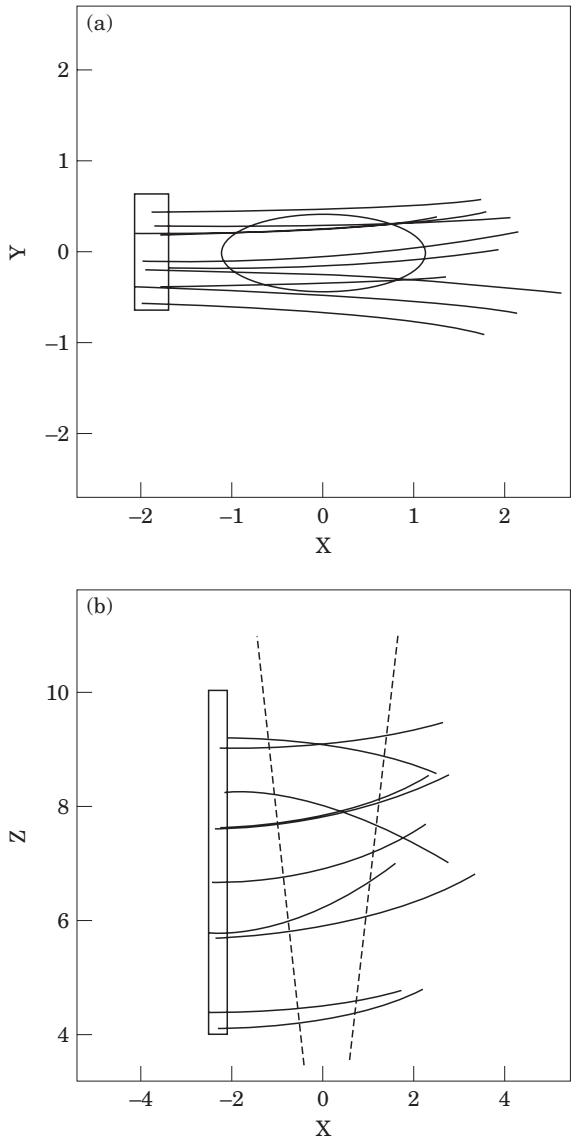

Figure 1. A selection of fish trajectories for simulated data. (a) The (x,y) cross-section of the $4° \times 10°$ beam is shown at a z-distance of 10 m by the ellipse. To the left of the beam cross-section, the rectangular box indicates the area in which the initial locations for all trajectories originate. The trajectories are indicated by the lines beginning in this box and travelling in the positive x-direction. Trajectories that pass through the beam cross-section may generate detected echoes in the simulated data. (b) The (x,z) cross-section of the beam at the $y=0$ plane is indicated by the dashed lines. The rectangular box indicates the region where trajectories originate. The same trajectories as shown in panel (a) are indicated by the lines beginning in this box and travelling in the positive x-direction.

to study the effects of spatial distribution and the total number of echoes on the estimation accuracy. We shall describe the process of generating the locations along a fish's trajectory.

We begin with the description of the simulation process for the $4° \times 10°$ transducer. First, the initial location, migration velocity, migration direction angles, and direction angle increments are obtained. Table 1 shows the input parameters used for simulated data for a $4° \times 10°$ transducer.

The initial location for the ith fish is given by:

$$x_{i,1} = -1.5z_{max}\tan\lambda_{max} - U(0, \mu+\sigma),$$

$$y_{i,1} = U(-1.5z_{max}\tan\nu_{max}, 1.5z_{max}\tan\nu_{max}), \quad (6)$$

$$z_{i,1} = U(-z_{min}, z_{max}).$$

where U(a,b) is the notation for a uniformly distributed random variable on the interval [a,b]. In Equation (6), we use the notation $x_{i,j}$ with $j=1$ to indicate the initial location of the ith fish.

Every 1/r seconds, the (x,y,z) location of the fish is updated, for a total of k_l pings. The updating process starts by generating an initial migration velocity magnitude, V, and migration direction angles, θ, φ, for each fish. These normally distributed random variables are given by:

$$V \sim N(\mu_\nu, \sigma_\nu^2),$$

$$\theta \sim N(\mu_\theta, \sigma_\theta^2), \quad (7)$$

$$\varphi \sim N(\mu_\varphi, \sigma_\varphi^2).$$

To allow for a curved trajectory, we increment the initial velocity direction angles θ and φ, with the incremental parameters δ_1 and δ_2. The incrementing process generates vectors $\theta_{i,j}$ and $\varphi_{i,j}$ of length k_l for each of the $i=1, \ldots, n$ fish being simulated. For the ith fish, the jth element of these vectors is given by

$$\theta_{i,j} = \delta_1 + \theta_{i,j-1},$$

$$\varphi_{i,j} = \delta_2 + \varphi_{i,j-1},$$

for $j=2, \ldots, k_l$. The initial elements come from the ith value of the random variables described in Equation (7). Next, migration velocity vectors can be calculated for each fish. These are defined for each of the Cartesian coordinates as:

$$V_{x,i,j} = V_i \sin\theta_{i,j} \cos\varphi_{i,j},$$

$$V_{y,i,j} = V_i \sin\theta_{i,j} \sin\varphi_{i,j},$$

$$V_{z,i,j} = V_i \cos\varphi_{i,j}, \quad (8)$$

where V_i is given by Equation (7). Finally, the coordinates of the ith fish trajectory are:

Table 1. Input parameters.

Parameter	Value	Description	Measurement units
μ_v	0.4	Mean migration speed	$m \times s^{-1}$
σ_v	0.03	s.d. migration speed	$m \times s^{-1}$
μ_θ	0	Mean first spherical coordinate	Degrees
σ_θ	1	s.d. first spherical coordinate	Degrees
μ_φ	90	Mean second spherical coordinate	Degrees
σ_φ	0.5	s.d. second spherical coordinate	Degrees
μ_{δ_1}	0	Mean first incremental value	Degrees
σ_{δ_1}	0.1	s.d. first incremental value	Degrees
μ_{δ_2}	0	Mean second incremental value	Degrees
σ_{δ_2}	0.5	s.d. second incremental value	Degrees
z_{min}	4	Minimum z-coordinate	m
z_{max}	10	Maximum z-coordinate	m
ν_{max}	2.4	Maximum up/down angle	Degrees
λ_{max}	6.4	Maximum left/right angle	Degrees
r	10	Ping frequency	$Pings \times s^{-1}$
n	50–2500	Number of fish	Fish
k_l	100	Number of pings per trajectory	Pings

$$x_{i,j} = x_{i,j-1} + \frac{V_{x,i,j-1}}{r},$$

$$y_{i,j} = y_{i,j-1} + \frac{V_{y,i,j-1}}{r},$$

$$z_{i,j} = z_{i,j-1} + \frac{V_{z,i,j-1}}{r},$$

for $j=2, \ldots, k_l$, with the initial locations given by Equation (6).

Examples of simulated trajectories illustrate how realistic fish traces can be generated by this process (Fig. 1). These trajectories all begin in an area of space with x-coordinates outside the beam and proceed in the positive x-direction. Note that the initial (x,y,z) coordinates, the initial slope, and the degree of curvature vary among trajectories. The trajectory lengths also differ, since the migration velocities are different and each trajectory is calculated for the same number of pings.

Once the trajectories have been generated by the process described above, the program uses a stochastic method to determine if a fish at each location in a trajectory will generate a detected echo. The detection process follows Equation (1), where p(x,y,z) is estimated using the procedures described in the section describing the estimation of the detection probability function. For individual fish, the detection probability sequence, p_l, $l=1, \ldots, k_l$, is obtained. To simulate random detection, a fish echo is classified as detected if $\tau<p_l$, where $\tau \sim U(0,1)$; otherwise, the fish is not detected at this location.

The trajectory simulation process is carried out for all n fish, i.e. $i=1, \ldots, n$. The simulated trajectories are classified as originating from either: tracked fish, if four or more detected echoes have been generated; untracked fish, for trajectories with less than four detected echoes; and undetected, for fish that pass through the beam but do not generate a detected echo. The number of each of these three types of events is tallied by the program. The total number of fish passing through the beam is the sum of these three components. Because of the random nature of the simulated trajectories, some trajectories do not pass through the beam. Therefore, the number of fish that pass through the beam is calculated as described above; it is not n.

The simulation program generates a data file that contains the locations and corresponding times for all of the detected echoes, plus a sequential fish number to group those echoes that come from each tracked fish. In a separate output file, the program records the mean upstream migration speed for the simulated fish in the data file and the total number of fish passing through the beam. The data file can then be used in the echo counting model to test the performance of the estimation procedures.

In the simulation process for our 8° transducer, the initial location settings for $y_{i,1}$ in Equation (6) is changed to:

$$y_{i,1} = U(-1.5 z_{max} \tan \nu_{max}, 0)$$

to emulate the fish behaviour at Spences Bridge, where the fish density was confined to the bottom half of the beam. Also the initial input parameters ν_{max} and λ_{max} in Table 1 are both set to 6° for this transducer.

A total of 100 data sets were generated by the simulation program using the input parameters listed in Table 1. The condition that the number of fish generated was distributed as $n \sim U(50, 2500)$ was imposed. This

resulted in the number of fish migrating through the beam ranging from 44 to 1511 for the 4° × 10° transducer (Fig. 2a) and from 21 to 869 for the 8° transducer (Fig. 2b).

Experimental comparison to visual estimate

An experiment was conducted on the Thompson River near Spences Bridge, British Columbia to compare acoustic estimates from the split-beam system with visual counts (Enzenhofer *et al.*, 1998). This site was chosen because it had a river cross-section that allowed acoustic measurements to be made readily and because the water clarity was sufficient to permit visual counting. The experiment was designed to allow simultaneous acoustic and visual observations as the fish passed through the beam. Visual counts were done in real-time and the fish were recorded on videotape. Real-time acoustic estimates were obtained from the automatic fish tracking software. Both a 4° × 10° elliptical beam and an 8° circular beam transducer were used (Fig. 3).

Fish migration rates ranged from ~400 to ~8000 fish h^{-1}. The acoustic system is unable to distinguish echoes from single-target sources when the target density becomes too high, which results in an increasing proportion of the echoes being removed by the single-target selection software as fish density increases. To avoid having this effect confounded with effects due to the echo counting model, only those observations with a visual count rate less than 1500 fish h^{-1} have been used.

Development of statistical procedures

The echo counting model estimates functions describing the spatial dependence of echo density, fish density, fish migration speed, fraction of fish migrating upstream, fish flux, and detection probability. All of these functions must be estimated from discrete observations. To do this, we used kernel density estimation and kernel regression, since these non-parametric techniques are well studied and can be used to describe a wide variety of distributions. The usual one-dimensional kernel density techniques were extended to three dimensions. The accuracy of the estimates was found to be highly dependent on the smoothing parameter, or bandwidth. (The term bandwidth is used here in the statistical sense of smoothing parameter. It is not to be confused with frequency bandwidth as used in acoustics and other wave propagation phenomena.) Therefore, for both kernel density and kernel regression, we have derived data-based smoothing parameters.

In practice, we have yet to use the feature of the echo counting model that specifies the fraction of fish migrating upstream, $\hat{f}_u(x,y,z)$. The data from the Spences Bridge experiment did not contain any fish migrating downstream. Typically at our site on the Fraser River we observe approximately 1–2% of the tracked fish identified as moving downstream. Consequently, there are too few observations to derive a meaningful spatial dependence for $\hat{f}_u$. The simulated data also did not contain any downstream migrants. In the sections below, we will ignore the estimation of this factor and assume that $\hat{f}_u = 1$ for all calculations.

Estimation of the cumulative echo density function

Detailed discussions of univariate kernel density estimation can be found in Silverman (1986); however, we require a three-dimensional kernel, with separate smoothing parameters for each dimension. Our decision to use separate smoothing parameters, rather than a global smoothing parameter for all dimensions, arises from our experience measuring acoustic targets held at fixed positions in the beam (Enzenhofer and Olsen, 1996). Data from these tests yield similar variances for the x- and y-dimensions, but a significantly smaller variance for the z-dimension. Independent smoothing parameter selection gives us a flexible way to account for this property.

The data from which e(x,y,z) is estimated consists of a set of coordinates (x_j,y_j,z_j), where $j = 1, \ldots, n_e$ indexes the locations at which an echo has been observed. The estimated three-dimensional kernel density function with different smoothing parameters is defined by:

$$\hat{f}(x,y,z) = \frac{1}{n_e} \sum_{j=1}^{n_e} \frac{1}{h_x h_y h_z} K\left(\frac{x - x_j}{h_x}, \frac{y - y_j}{h_y}, \frac{z - z_j}{h_z} \right) \qquad (9)$$

where n_e is the number of total observed echoes, $K(\cdot)$ is the kernel function described in detail in Silverman (1986), and h_x, h_y, h_z are the smoothing parameters in each direction. The choice of smoothing parameters is crucial when applying non-parametric density estimators. Detailed discussions for the univariate case can be found in Park and Marron (1990), Sheather and Jones (1991) and Jones *et al.* (1996). Silverman (1986) discusses multivariate kernel density estimation and gives an estimate for a global smoothing parameter, i.e. assuming that the smoothing parameters in each direction are equal.

The data-based independent smoothing parameters for the density estimator Equation (9) can be derived (details can be requested from the authors) by minimizing the mean integrated square error (MISE) of $\hat{f}(x,y,z)$, since the MISE is a commonly used criterion for evaluating the goodness-of-fit for this estimator. It can be

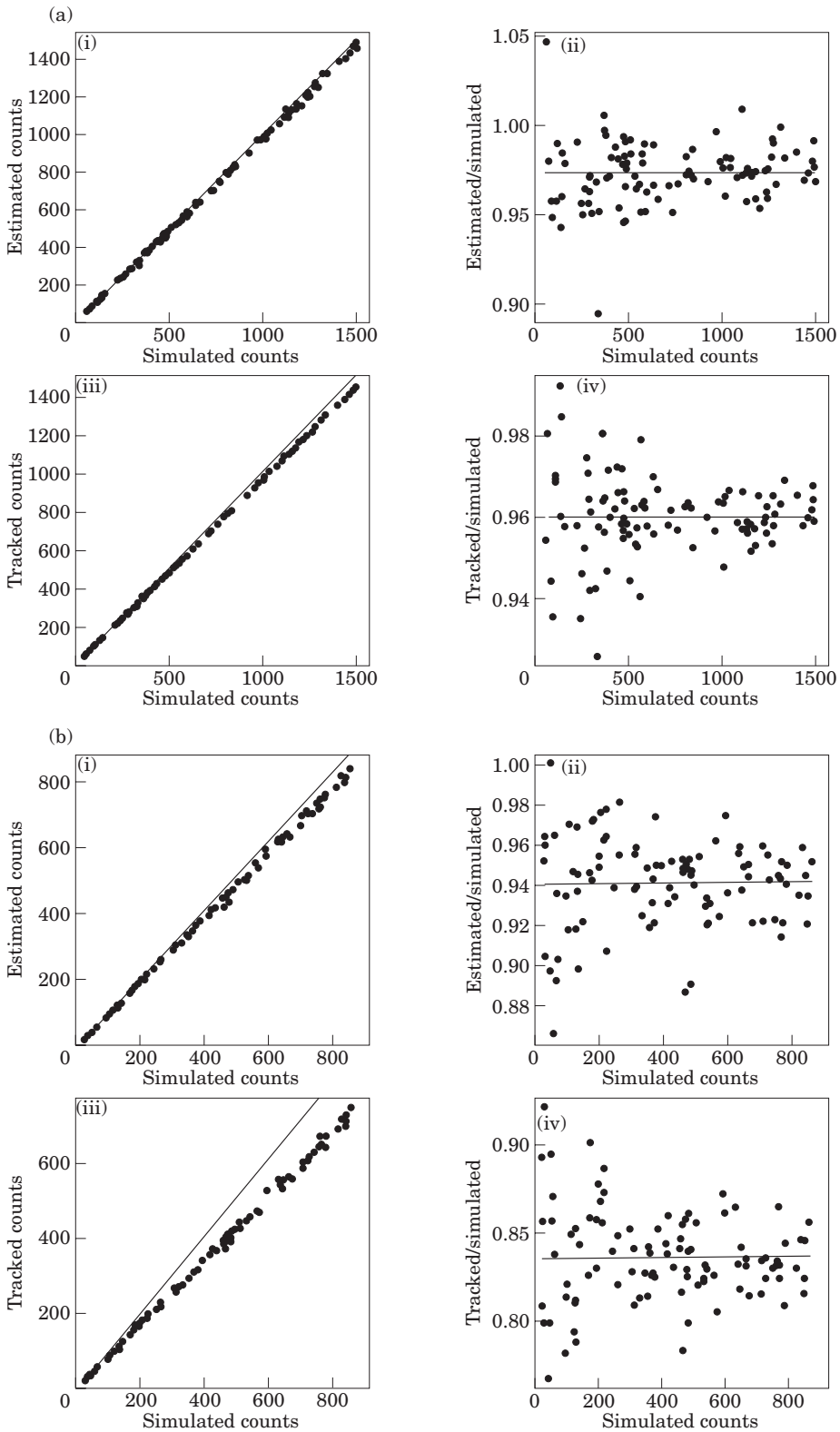
(a)
(i)
Estimated counts
Simulated counts
(ii)
Estimated/simulated
Simulated counts
(iii)
Tracked counts
Simulated counts
(iv)
Tracked/simulated
Simulated counts
(b)
(i)
Estimated counts
Simulated counts
(ii)
Estimated/simulated
Simulated counts
(iii)
Tracked counts
Simulated counts
(iv)
Tracked/simulated
Simulated counts

shown that the smoothing parameter estimates can be expressed as

$$h_x = C \times \min(\hat{\sigma}_x, R_x/1.34)\, n_e^{-1/7},$$

$$h_y = C \times \min(\hat{\sigma}_y, R_y/1.34)\, n_e^{-1/7},$$

$$h_z = C \times \min(\hat{\sigma}_z, R_z/1.34)\, n_e^{-1/7}, \quad (10)$$

where R_x, R_y, and R_z are the interquartile ranges from x_j, y_j, and z_j, and $\hat{\sigma}_x$, $\hat{\sigma}_y$ and $\hat{\sigma}_z$ are the estimated standard deviation from x_j, y_j and z_j, respectively. The constant C is from table 3.1 in Silverman (1986) and $\min(a_1, a_2)$ denotes the minimum value of a_1, a_2.

Kernel density estimation generates a probability density function, which must integrate to one over the entire volume occupied by the observations. In our case the cumulative echo function should integrate to the total number of observed echoes; therefore, we require that:

$$\iiint \hat{e}(x,y,z)\,dx\,dy\,dz = n_e,$$

so that the estimate for the cumulative echo density is given by:

$$\hat{e}(x,y,z) = n_e \times \hat{f}(x,y,z). \quad (11)$$

Estimation of the detection probability function

Estimation of detection probability, p(x,y,z), used data from an experiment with a dead sockeye salmon as the acoustic target. A set of discrete measurements, $p_i(x_i,y_i,z_i)$, $i = 1, \ldots, d_p$, was obtained by placing the fish at d_p separate locations (x_i,y_i,z_i) in the beam, each location indexed by i. The number of pings transmitted, I_i, and the number of echoes detected, n_i, were recorded for each location. The discrete detection probabilities can then be defined as:

$$p_i(x_i,y_i,z_i) = \frac{n_i}{I_i} \qquad i = 1, \ldots, d_p.$$

We describe the dependence of the detection probability as a function of the beam pattern factor (bpf) rather than as a function of the coordinates. This allows the reduction of a three-dimensional problem to one dimension. The (x,y,z) values from each of the i locations, were

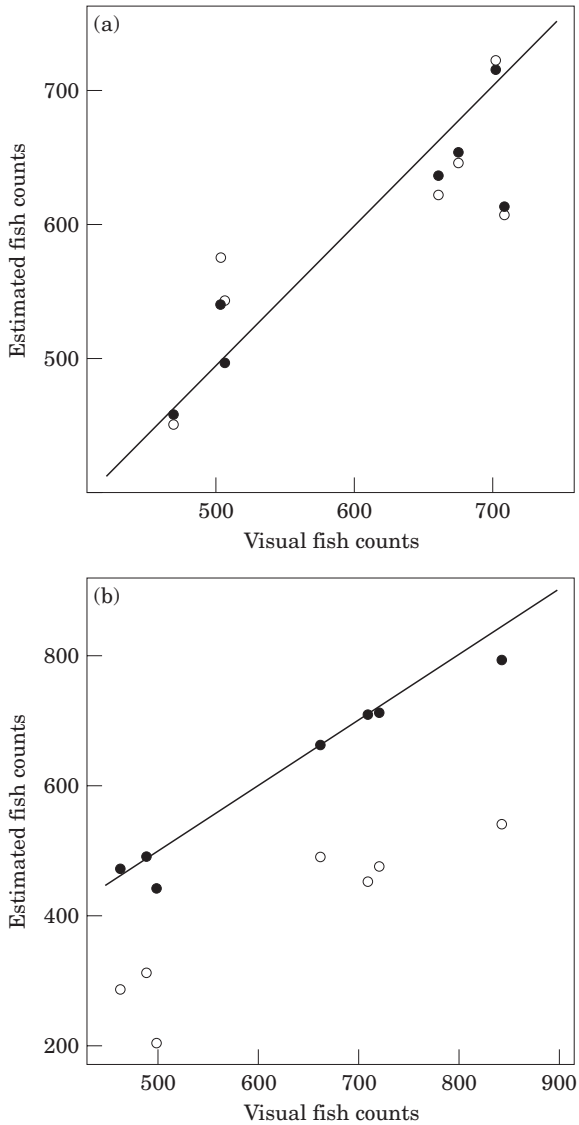

Figure 3. Data from the experiment at Spences Bridge. (a) The echo counting model estimates for the 4° × 10° transducer are plotted with solid dots, while the estimates from the real-time tracking program are plotted as open circles. The line represents equal values of estimated count vs. visual count. Only those data sets with hourly migration rates less than 1500 fish h^{-1} are shown. (b) The same plot as in panel (a) is shown for the 8° transducer. Again, only migration rates less than 1500 fish h^{-1} are shown. For this case, the tracked estimates are much lower than the visual count, while the counting model estimates are significantly less biased.

Figure 2(a). Comparison of the echo counting model estimates 4° × 10°, the tracked fish counts and the true fish numbers for 100 sets of simulated data. Simulated data sets were generated that covered a range of 44–1511 fish. (i) Model estimates vs. simulated fish numbers are shown by the points. The line represents equal values of estimate vs. simulated value. (ii) The ratio of estimated to simulated is shown vs. simulated fish number. The line shows the mean value of this ratio. (iii) Simulated fish number vs. tracked count is shown by the points. The line represents equal values of simulated vs. tracked. (iv) The ratio of tracked to simulated is shown by the points. The line shows the mean value of this ratio.

Figure 2(b). The same comparison for 8° transducer.

used to calculate the corresponding up/down angle, ν, and left/right angle, λ, from the acoustic coordinate system described in the Appendix. Then the two-way beam pattern factor (in units of decibells) was approximated by:

$$bpf \approx bpf_v + bpf_h \tag{12}$$

where:

$$bpf_v = c_{v_0} + c_{v_1}v + c_{v_2}v^2 + c_{v_3}v^3 + c_{v_4}v^4,$$

$$bpf_h = c_{h_0} + c_{h_1}\lambda + c_{h_2}\lambda^2 + c_{h_3}\lambda^3 + c_{h_4}\lambda^4.$$

Values for the coefficients c_v and c_h were obtained from calibration of the transducers. For example, the coefficients for the 4° × 10° transducer are:

$$c_v = (0, -0.002998, -1.323180, 0.078200, -0.029784),$$

$$c_h = (0, 0.000275, -0.317320, 0.002170, -0.001179)$$

This process yields a data structure (bpf_i, p_i), $i=1, \ldots, d_p$ with the detection probability p being a dependent function of the beam pattern factor, bpf, as:

$$p_i = f(bpf_i) + \varepsilon_i, \tag{13}$$

where ε_i are i.i.d with mean 0 and variance σ_p^2, i.e. $\varepsilon_i \sim (0, \sigma_p^2)$. Then p(bpf) can be estimated by a one-dimensional kernel regression technique. The estimate for Equation (13) is defined as:

$$\hat{f}(pbf) = \frac{\Sigma_{i=1}^{n} K\left(\frac{bpf - bpf_i}{h}\right) p_i}{\Sigma_{i=1}^{n} K\left(\frac{bpf - bpf_i}{h}\right)} \tag{14}$$

where K(·) is the kernel function and h is the smoothing parameter or bandwidth. The selection of smoothing parameter is pivotal for accurate estimation. This issue has been extensively discussed in the literature; see, for example, Nychka (1991) and Gasser *et al.* (1991). A data-dependent smoothing parameter for this regression (details can be requested from the authors) using the mean integrated square error (MISE) for $\hat{f}(bpf)$ can be expressed as:

$$\hat{h} = \left\{ \frac{\hat{\sigma}_p^2}{\frac{2\sqrt{\pi}}{\hat{b}^3}\frac{[\max(bpf_i) - \min(bpf_i)]}{30}\frac{1 + 5e^{\hat{a}} - 5e^{2\hat{a}} + 15e^{3\hat{a}}}{(1+e^{\hat{a}})^5}} \right\}^{1/5} d_p^{-\frac{1}{5}}, \tag{15}$$

where $\hat{\sigma}_p^2$ is the estimated variance of the p_i, e is the base of the natural system of logarithms ($e \approx 2.718$), and $\hat{a}$ and $\hat{b}$ are obtained from a logistic regression between p_i and bpf_i.

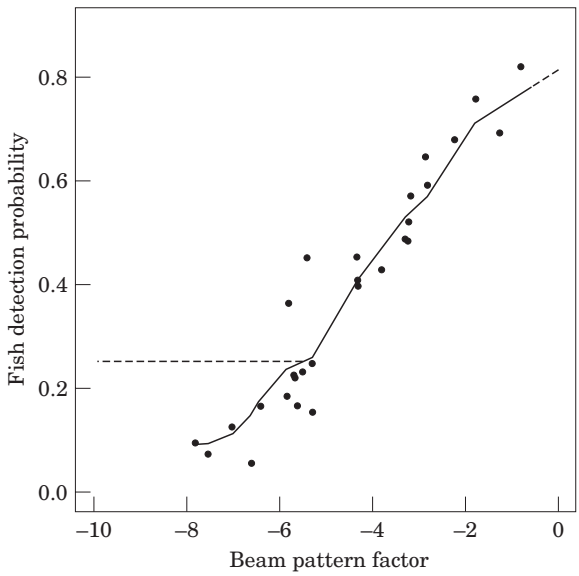

Figure 4. The fish echo detection probability is plotted as a function of beam pattern factor (measured in dB). These data are for a 8° transducer with a sockeye salmon used as the target. The solid line represents the kernel regression fit to the data. The dashed line represents extrapolation (for values near beam pattern factor of 0) or truncation (for values of beam pattern factor less than −5.5). The detection probability has been truncated to 0.25 for use in the echo counting model, while for the simulation program, this truncation is not used.

To estimate the detection probability function, p(x,y,z), for a fish, first the bpf for that location is calculated using the procedures described above. If the calculated bpf falls within the range of the observed bpf_i, linear interpolation is used to calculate detection probability. Since we do not have an analytic representation for p as a function of bpf; rather, we have d_p discrete values of $p(bpf_i)$, we have to interpolate these values. If bpf is greater than the maximum of the observed bpf_i, linear extrapolation is used. If bpf is less than some minimum value we have chosen, p(x,y,z) is defined to be 0.25 (Fig. 4). Thus, we truncated the lower limit of p to be 0.25. This truncation was required to give reliable estimates for the fish density function, ρ(x,y,z) and is a result of sampling small numbers of echoes to estimate both e and p. Equation (3) shows how, when both $\hat{e}$ and $\hat{p}$ become smaller as we get near the edge of the beam, $\hat{\rho}$ can begin to vary widely. This truncation process helped stabilize our estimates for ρ while maintaining a small relative bias.

Estimation of the fish speed function

The acoustic system includes fish tracking software. The tracking algorithm works well when a single fish is in the beam. However, if several fish are in the beam and are separated by a small difference in range, the algorithm

can confuse the trajectory of one fish with that of another. The resulting trajectories do not give accurate information about the movement of fish through the beam. We apply a selection criterion to choose only well-tracked fish from the group of all tracked fish. Only the locations (x_u,y_u,z_u), $u=1, \ldots, n_u$, $n_u<n_e$ from these well-tracked single fish, and the corresponding time for each observed echo, are used to estimate the fish migration speed, S. Suppose that the ith fish, where $i=1, \ldots, k_f$, is detected n_i times and its jth tracked position and time are written as $(x_{i,j},y_{i,j},z_{i,j},t_{i,j})$ where $j=1, \ldots, n_i$, with $\Sigma_{i=1}^{k_f} n_i=n_u$. Our experience has led us to use the correlation coefficient of $x_{i,j}$ vs. $t_{i,j}$ as an indicator to select a subset of well-tracked fish. The criterion is to choose fish trajectories with a correlation coefficient greater than 0.75.

We are only concerned with the fish migration speed in the x-direction to obtain the upstream fish flux. Therefore, for each of the selected fish, the $x_{i,j}$ vs. $t_{i,j}$ trajectory is fit using a robust regression procedure introduced by Huber (1973). This procedure estimates the parameters τ_i and s_i from the regression equation:

$$x_{i,j}=\tau_i+s_i t_{i,j}, \quad j=1, \ldots, n_i. \tag{16}$$

The associated fish speed is predicted from this regression by $\hat{s}_i$, since:

$$\hat{s}_i=\frac{\hat{x}_{i,j}-\hat{x}_{i,j-1}}{t_{i,j}-t_{i,j-1}}. \tag{17}$$

where $\hat{x}_{i,j}$ and $\hat{x}_{i,j-1}$ are the predicted values from the regression Equation (16).

The echo counting model described in Mulligan and Kieser (1996) used an estimated functional form $\hat{S}(x,y,z)$, to describe the systematic spatial variation in fish migration speed. We discovered that, after selecting only well-tracked fish, there were too few observations of $\hat{s}_i$ to make reliable estimates of S. Therefore, we have simplified this procedure to calculation of a weighted mean speed, given by:

$$\hat{S}=\frac{\Sigma_{i=1}^{k_f} n_i\hat{s}_i}{\Sigma_{i=1}^{k_f} n_i}=\frac{\Sigma_{i=1}^{k_f} n_i\hat{s}_i}{n_u}. \tag{18}$$

Results

Simulated data

Simulated data was used to determine the variance and bias of the estimated number of fish migrating through the beam, $\hat{N}$, and to refine our estimation procedures. The $4^\circ \times 10^\circ$ transducer data gave very similar results for the ratio of counting model estimate to simulated count and the ratio of tracked estimate (obtained from the simulation program as described earlier) to simulated count (Table 2). However, the 8° transducer results are quite different for counting model estimates vs. tracking estimates. This difference is due to the decreased tracking efficiency near the edge of the beam and is exacerbated by the circular cross-section of the 8° beam. The counting model estimate has almost the same relative bias for both transducers.

Table 2. Mean and standard deviation (s.d.) for the ratio from 100 simulated data.

Transducer	$4^\circ \times 10^\circ$		8°	
Ratio	Mean	s.d.	Mean	s.d.
Estimated to simulated	0.9731	0.0175	0.9408	0.0221
Tracked to simulated	0.9600	0.0098	0.8361	0.0256

The model performance with simulated data is dependent on the choice of input parameters and the initial fish distribution generated by Equation (6). The values used in these simulations generate fish trajectories that are uniformly distributed in the y and z dimensions and span the entire beam cross-section for the simulated $4^\circ \times 10^\circ$ data. If the range of y were to be limited to produce trajectories in only the lower portion of the beam to simulate high fish density near the river bottom, as was done for the simulated 8° data, then the percentage of untracked and undetected fish increase, since p is low near the edge of the beam. This in turn, affects the bias and standard deviation of $\hat{N}$. Thus, the bias and variance of the echo counting model estimates depend on the distribution of $\rho(x,y,z)$.

We anticipated that the accuracy of the estimated number of fish would be dependent on the total number of fish in the simulation. When the number of observations is low, it should be more difficult to estimate the spatial dependence of $e(x,y,z)$ and $\rho(x,y,z)$. However, the ratio of the model estimate to the simulated number of fish is quite stable, even when the total number of fish is as low as 150 (Fig. 2aii, 2bii). Perhaps this is because the kernel density estimation uses smoothing parameters that vary as $n_e^{-1/7}$, where n_e is the number of echoes. Changing the size of the smoothing parameter increases the size of the local neighborhood used to estimate the density, as the number of echoes decreases. Thus, for smaller numbers of echoes, the smoothing parameters are larger and the resulting relative bias remains stable.

Experimental data

The experiment conducted at Spences Bridge on the Thompson River compared model estimates to visual estimates. A total of 14 data sets, seven from the $4^\circ \times 10^\circ$ transducer and seven from the 8° transducer, with visual counts less than 1500 fish h^{-1}, were selected from this experiment to test the model. Table 3 lists the visual

Table 3. Summary of data from Spences Bridge experiment.

For 4° × 10° transducer			For 8° transducer		
Visual	Tracked	Estimated	Visual	Tracked	Estimated
470	458	464	465	286	472
504	579	545	721	475	713
678	646	654	500	203	443
507	547	502	664	490	663
710	609	615	844	539	794
663	623	637	710	451	710
705	721	715	490	314	491

Table 4. Bias point and interval estimate (C.I.) for Spences Bridge experiment.

Transducer Bias	4° × 10°			8°		
	Point	C.I.	s.d.	Point	C.I.	s.d.
Estimated to visual	0.9788	(0.9200, 1.0413)	0.0647	0.9749	(0.9320, 1.0198)	0.0462
Tracked to visual	0.9925	(0.9079, 1.0848)	0.0962	0.6104	(0.5125, 0.7269)	0.1019

counts (Visual), the tracked fish number (Tracked) from the real-time fish tracking algorithm, and the estimated counts (Estimated) from the echo counting model.

All of the estimates in Table 3 are subject to error. Following the procedures from Schnute *et al.* (1990), the maximum likelihood point and interval estimate for the relative bias of the ratios between the model estimates to visual counts and tracking estimates to visual counts, are summarized in Table 4.

For the 4° × 10° transducer, both the model estimate and the tracking estimate are not statistically significantly different from the visual count. However, the echo counting model estimates have smaller standard deviation than the real-time tracked estimates. This indicates that the echo counting model estimates are more precise than the real-time tracking estimates. This property can be also seen from Figure 3(a). For the 8° transducer, the model estimate is not statistically significantly different from the visual count, but the real-time tracking estimate is significantly different (Fig. 3b). Comparison of Table 4 and Table 2 demonstrate that the standard deviations of the relative bias are larger for the Spences Bridge data than for simulated data.

Discussion

In this paper we describe the development of statistical procedures that are required to apply the echo counting model of Mulligan and Kieser (1996) to real or simulated data. We found that three-dimensional kernel density estimation of the cumulative echo distribution, e(x,y,z), was successful when it included independent, data-based smoothing parameters for each dimension. In addition, kernel regression worked well to estimate the dependence of fish detection probability, p, on position in the beam. Here again, a data-based smoothing parameter proved necessary to obtain accurate estimates. In this latter instance, we have not included any dependence of detection probability on distance from the transducer, R; rather we limited our description to the angular variables ν and λ. The reason for excluding R-dependence was due to the fact that, at our site on the Fraser River, all of the upstream fish movement occurs between 3–15 m from the transducer. At this close range, R-dependence is not significant; whereas, if we observed fish movement out to a larger range, for example 100 m, we would expect p to show some R-dependence.

For the 4° × 10° transducer, both the model estimates and the real-time tracking estimates for the Spences Bridge data were found not to be statistically significantly different; whereas, the real-time tracking estimates for the 8° transducer were statistically significantly different from the model estimates. If the fish tracking algorithm accurately estimates the number of fish passing through the beam that generate four or more echoes (recall that four echoes are a prerequisite for the tracking algorithm), a larger bias is to be expected for tracked fish estimates than for echo counting estimates. This is because some fish will have passed through the beam and generated three or less echoes, while some will generate no echoes at all. This phenomenon can lead to a substantial underestimate of the number of migrating fish, as demonstrated by the tracking estimates for the 8° transducer. The echo counting model accounts for these two possibilities and, therefore, should give a smaller

bias. This improvement is particularly evident for the 8° transducer data.

The real-time tracking estimates are reasonably accurate for the 4° × 10° transducer. This result is dependent on the ping rate used. If too low a ping rate is used, many fish will pass through the beam without being detected the minimum number of times required by the tracking algorithm. The Spences Bridge data were obtained with the acoustic system configured to record echo data between the ranges of 3.5–8.5 m. At these short ranges, the relatively high frequency of 10 pings × s^{-1} is a good choice. If fish at long ranges are to be observed, a slower ping rate might be necessary. Data obtained over a wide interval, from short to long range, might have to be acquired in two or more stages, each stage having a different ping rate, if accurate tracked-fish estimates are to be obtained.

One difference between the simulated and real data is that, in the simulation program, tracking works perfectly. That is, all fish that produce four or more echoes are accurately counted. The real-time tracking of real data does not achieve this perfect goal. It is much more difficult to track many fish simultaneously, especially when they differ in range by a small amount. In practice, our real-time algorithm over- and underestimates the number of fish for different trajectories. This phenomenon is difficult to reproduce with simulated data.

The fish flux rates observed in the Spences Bridge experiment ranged from ~400 to ~8000 fish h^{-1}. While these are not unusual for the Fraser River system, they are much higher than most salmon bearing rivers experience. A more typical river system might be expected to have less than 2000 fish h^{-1}. In our comparison with the data from Spences Bridge, we examined only those observations with fluxes $\leq$1500 to avoid problems imposed by the acoustic detection and tracking software, not because of limitations of the echo counting model. Therefore, we believe that this model should be used for providing estimates to help with the management and understanding of many salmon fisheries.

We assume that the fish distributions and behaviour reflected in the Spences Bridge data are representative of typical data from the Fraser River, where we intend to apply the echo counting model to help with the management of the sockeye salmon fishery. Therefore, the real-time tracking and echo counting model estimates for Fraser River data should be similar to those obtained here.

While working with simulated data, we noticed that our estimated migration speed, $\hat{S}$, was negatively biased. This is due to the fact that migration speed is estimated using only well-tracked fish, which do not comprise a random sample. Fish that swim quickly through the beam are more likely to generate fewer echoes than fish that swim more slowly. Once again, the requirement of four or more echoes per tracked fish will tend to yield a sample that is biased towards the slower swimming individuals. An examination of the magnitude of this bias for the Spences Bridge data (mean fish speed of 0.4 ms^{-1} and coefficient of variation of 0.075) demonstrates that the bias should be less than 2% (Fig. 5).

A criticism of the model that followed the publication of Mulligan and Kieser (1996), was that ρ and S should be correlated, so that Equation (4) is incorrect. Specifically, this equation assumes that:

$$\widehat{\rho S} \approx \hat{\rho}\hat{S}. \tag{19}$$

This approximation will only be valid if the correlation between ρ and S is negligibly small. Consider the echo data, $(x_{i,j},y_{i,j},z_{i,j})$ where i indexes fish and j indexes the echoes within a trajectory from an individual fish. If we choose a specific value of i, the distance between coordinates $x_{i,1}$, $x_{i,2}$, ... must be correlated to $S_{x,i}$, the x-component of the migration speed of fish i. The same is true for the y- and z-coordinates with their respective speed components. Therefore, ρ must also be correlated to S for this case. By contrast, a set of the x-coordinates among fish, for example $x_{i,1}$ where i=1, 2, ... are uncorrelated as required by Equation (6) for simulated data and as assumed for real data. The same holds true for the migration speeds among fish as required by Equation (7) for simulated data and as assumed for real data. When evaluating Equation (3), ρ(0,y,z) has been estimated within a small region of space defined by the magnitude of the kernel density smoothing parameters. Consider two scenarios for this region. First, the number of individual fish is small and the mean number of echoes within each fish's trajectory is large. For this case, we would expect the coordinates to be correlated and Equation (19) would not be valid. The second scenario is for the case where the region contains echoes from a large number of fish with only a single echo from each fish. In this latter case, Equation (19) should be a good approximation. We believe the second scenario is closer to the real situation than the first. The accuracy of the echo counting model estimates for both the simulated and the Spences Bridge data support this assumption.

Echo counting is more susceptible to random echoes from non-fish sources than echo tracking. This is because tracking uses additional signal processing to require systematic behaviour among the related echoes within a fish trajectory. This additional processing acts like a filter to block random echoes and pass systematically related echoes. Many of these random echoes can be removed from the data by an experienced person. Several noise sources, such as boat wakes or downstream floating debris, are easily identified from an echogram and can be removed. This data editing process

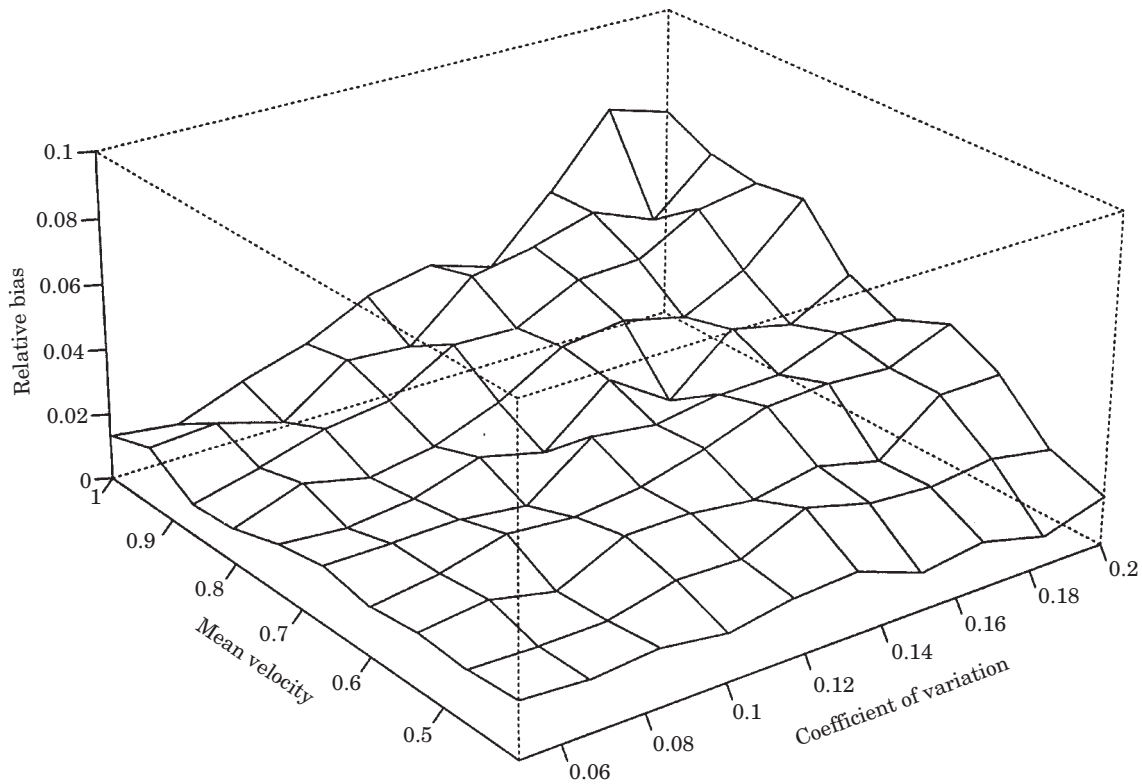

Figure 5. The relative bias in the migration speed estimate is plotted vs. the mean migration speed and the coefficient of variation (c.v.) of the speed for simulated data. As the velocity and the c.v. increase, the relative bias in the estimated speed increases. The estimated speed underestimates the true speed as described in the text.

has been applied to all of the data from the Spences Bridge experiment.

We are encouraged by the performance of the echo counting model and believe that it will provide estimates that are useful for managing salmon fisheries. The level of accuracy of the results presented here is the result of careful acoustic measurements and the successful development of appropriate statistical procedures to estimate fish density and migration speed. We hope that these acoustic techniques will be adopted by agencies responsible for the management of salmon fisheries.

Acknowledgements

The authors wish to thank Dr Robert Kieser and Dr Rick Routledge for reading early versions of this paper and providing many helpful comments. We also wish to thank two anonymous referees who provided several suggestions for clarifying and improving the text.

References

Enzenhofer, H. J., and Olsen, N. 1996. A reference target frame and fish deflection weir for fixed-location riverine hydroacoustic systems. Canadian Technical Report of Fisheries and Aquatic Sciences, 1996: No. 2347.

Enzenhofer, H. J., Olsen, N., and Mulligan, T. J. 1998. Fixed-location riverine hydroacoustics as a method of enumerating migrating adult Pacific salmon: comparison of split-beam acoustics vs. visual counting. Aquatic Living Resources, 11(2): 61–74.

Gasser, T., Kneip, A., and Kohler, W. 1991. A flexible and fast method for automatic smoothing. Journal of the American Statistical Association, 86: 643–652.

Jones, M. C., Marron, J. S., and Sheather, S. J. 1996. A brief survey of bandwidth selection for density estimation. Journal of the American Statistical Association, 91: 401–407.

Huber, P. J. 1973. Robust regression: asymptotic, conjectures, and monto carlo. Annals of Statistics, 1: 799–821.

Mulligan, T., and Kieser, R. 1996. A split-beam echo counting model for riverine use. ICES Journal of Marine Science, 53: 403–406.

Nychka, D. 1991. Choosing a range for the amount of smoothing in nonparametric regression. Journal of the American Statistical Association, 86: 653–664.

Park, B. U., and Marron, J. S. 1990. Comparison of data-driven bandwidth selectors. Journal of the American Statistical Association, 85: 66–72.

Schnute, J. T., Mulligan, T. J., and Kuhn, B. R. 1990. An error-in-variable bias model with an application to salmon hatchery data. Canadian Journal of Fisheries and Aquatic Sciences, 47: 1453–1467.

Sheather, S. J., and Jones, M. C. 1991. A reliable data-based bandwidth selection method for kernel density estimation. Journal of Royal Statistical Society, B 53: 683–690.

Silverman, B. W. 1986. Density Estimation for Statistics and Data Analysis. Chapman and Hall, London.

Appendix

The Cartesian (x,y,z) and split-beam (R,ν,λ) coordinates are related by the following transformations (Fig. 6):

$R^2=x^2+y^2+z^2$,

$x=z\tan\lambda$,

$y=z\tan\nu$,

$z=R\cos\Phi$,

$\Phi=\tan^{-1}\sqrt{\tan^2(\nu)+\tan^2(\lambda)}$,

where:

ν is the up/down angle,
λ is the left/right angle,
Φ is the off-axis angle,
x is the distance in the upstream/downstream direction,
y is the distance in the river surface/bottom direction,
z is the distance in the acoustic beam axis direction,
R is the distance of the fish from the acoustic transducer face.

Transformations between Cartesian (x,y,z) and spherical coordinates (R,θ,φ) are (Fig. 7):

$x=R\sin\theta\cos\varphi$,

$y=R\sin\theta\sin\varphi$,

$z=R\cos\varphi$.

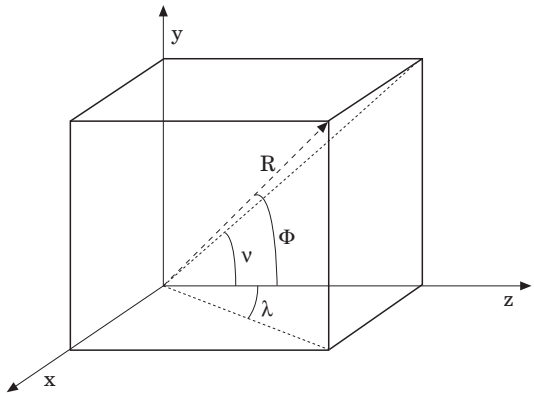

Figure 6. The Catesian (x,y,z) and split-beam (R,ν,λ) coordinate system.

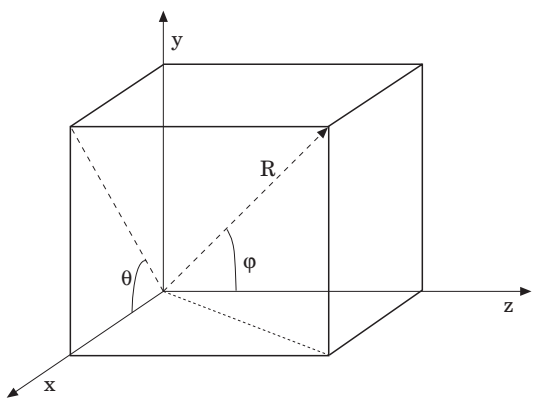

Figure 7. The Catesian (x,y,z) and spherical (R,θ,φ) coordinate system.